ISSN 0021-3640, JETP Letters, 2020, Vol. 111, No. 3, pp. 183–187. © Pleiades Publishing, Inc., 2020.
Russian Text © The Author(s), 2020, published in Pis'ma v Zhurnal Eksperimental'noi i Teoreticheskoi Fiziki, 2020, Vol. 111, No. 3, pp. 197–202.

CONDENSED MATTER

Ferromagnetic Resonance Study of Biogenic Ferrihydrite Nanoparticles: Spin-Glass State of Surface Spins

S. V. Stolyar[a, b, c, *], D. A. Balaev[a, c], V. P. Ladygina[b], A. I. Pankrats[a, c], R. N. Yaroslavtsev[a, b, c], D. A. Velikanov[a], and R. S. Iskhakov[a]

[a] *Kirensky Institute of Physics, Federal Research Center KSC, Siberian Branch, Russian Academy of Sciences, Krasnoyarsk, 660036 Russia*

[b] *Federal Research Center KSC, Siberian Branch, Russian Academy of Sciences, Krasnoyarsk, 660036 Russia*

[c] *Siberian Federal University, Krasnoyarsk, 660041 Russia*

**e-mail: stol@iph.krasn.ru*

Received November 14, 2019; revised December 31, 2019; accepted December 31, 2019

Ferrihydrite nanoparticles (2–3 nm in size), which are products of the vital activity of microorganisms, are studied by the ferromagnetic resonance method. The "core" of ferrihydrite particles is ordered antiferromagnetically, and the presence of defects leads to the appearance of an uncompensated magnetic moment in nanoparticles and the characteristic superparamagnetic behavior. It is established from the ferromagnetic resonance data that the field dependence of the frequency is described by the expression $2\pi\nu/\gamma = H_R + H^A_{(T=0)}(1 - T/T^*)$, where γ is the gyromagnetic ratio, H_R is the resonance field, $H_A \approx 7$ kOe, and $T^* \approx 50$ K. The induced anisotropy H^A is due to the spin-glass state of the near-surface regions.

DOI: 10.1134/S0021364020030145

1. INTRODUCTION

Interest in the study of antiferromagnetic nanoparticles is caused by fundamentally new properties of these objects [1, 2]. If a bulk antiferromagnet can be considered as a "weakly magnetic" material, the surface defects play an increasing role in the magnetic behavior when the particle size decreases. The presence of defects leads to the appearance of an uncompensated magnetic moment in an antiferromagnetic nanoparticle reaching hundreds of Bohr magnetons [2–9] and to effects associated with a superparamagnetic behavior: a magnetic hysteresis loop and the presence of a superparamagnetic blocking temperature [4–8], and so on. In addition, surface spins can form a separate magnetic subsystem, which can significantly affect the magnetic properties of a system of nanoparticles [10].

Ferrihydrite with a nominal formula $Fe_2O_3 \cdot nH_2O$, which is discussed in this work, plays an important role in the metabolism of living organisms. It is formed in the core of the ferritin protein complex, which is a capsule of the protein apoferritin. The size of ferrihydrite nanoparticles is in a narrow range of up to 8 nm. The transformation $Fe_2O_3 \cdot nH_2O \rightarrow FeOOH$ occurs as the particle sizes increase [11]. The majority of magnetic studies were performed on ferritin (horse spleen ferritin) [4, 5] and ferrihydrite obtained chemically [6, 7, 11–14]. According to neutron [12] and magnetometric [7] studies, ferrihydrite is an antiferromagnet with a Néel temperature of ≈350 K [12]. The superparamagnetic blocking temperature can vary up to ~100 K depending on the origin and size of the nanoparticles. At low temperatures, the magnetization curves are characterized by magnetic hysteresis and exchange bias (after cooling in an external field) [4–6, 15]. The temperature dependences of the coercivity and exchange bias fields are usually correlated [5, 6]. The effect of the exchange bias, which consists in the appearance of induced magnetic anisotropy, implies the presence of at least two interacting magnetic subsystems within one nanoparticle. The authors of [5, 6] attributed the observed effect of the exchange bias to the appearance of a spin-glass state of surface spins. In this case, the freezing temperature of surface spins (also manifested in anomalies in the temperature dependences of the magnetization [5, 6]) is usually much lower than the superparamagnetic blocking temperature.

It is reasonable that a spin glass-like state should also be manifested under magnetic resonance conditions. The resonance properties of ferrihydrite nanoparticles were studied in [13, 16–18]. The resonance curves at low temperatures are characterized by nonmonotonic temperature dependences and additional absorption lines [13, 16, 17]. However, an unambiguous relationship between resonance absorp-

tion and freezing of the surface-spin subsystem has not been established. Thus, despite a considerable number of studies of ferrihydrite and ferritin by various methods, a clear identification of the contribution of the surface-spin subsystem is an urgent task. In this work, we study the magnetic resonance of ferrihydrite nanoparticles. It is shown that the interaction of the surface spin subsystem with the antiferromagnetic "core" of particles is manifested in the temperature evolution of the frequency dependence of the resonance field.

2. TECHNIQUES

Ferrihydrite nanoparticles that are products of the vital activity of microorganisms *Klebsiella oxytoca* were studied. Under anaerobic conditions, this bacterial species can synthesize a secretory exopolysaccharide, Fe–EPS [19–21], which is associated with ferrihydrite nanoparticles. Bacteria *Klebsiella oxytoca*, which were extracted from sapropel taken from Lake Borovoe in Krasnoyarsk krai, were grown on a mineral-salt medium. Iron citrate was used as a source of carbon and energy. To obtain a sol of ferrihydrite nanoparticles, sediments of a bacterial culture containing nanoparticles were destroyed by ultrasound and washed with water, acetone, and 20% NaOH [22, 23]. The resulting sol of ferrihydrite nanoparticles in an aqueous solution was subsequently dried. Thus, the object of the study was ferrihydrite nanoparticles coated with an organic shell [24].

Electron microscopy studies of the resulting nanoparticles were carried out on a Hitachi HT7700 transmission electron microscope (accelerating voltage of 100 kV). The sizes of the studied nanoparticles were 2–3 nm. Static magnetic measurements (temperature dependences of the magnetization $M(T)$) in the zero field cooling (ZFC) and field cooling (FC) modes were carried out on a SQUID magnetometer [25]. Magnetic resonance studies were carried out using an original setup [26] making it possible to obtain field dependences of the frequency $\nu(H)$ in a wide range of fields, frequencies, and temperatures. The structure and magnetic properties of biogenic ferrihydrite nanoparticles were studied in [27–33].

3. RESULTS AND DISCUSSION

Figure 1 shows the dependences $M(T)$ for the studied sample of ferrihydrite nanoparticles in ZFC and FC modes in the fields of 0.1 and 1 kOe. The dependences $M(T)_{ZFC}$ demonstrate a pronounced maximum whose position is shifted toward lower temperatures with increasing field (for a field of 0.1 kOe, T_{max} is ≈25 K). The dependences $M(T)_{ZFC}$ and $M(T)_{FC}$ diverge near T_{max} and the divergence increases with decreasing temperature. This behavior is typical of superparamagnetic blocking processes, and the temperature T_{max} can be considered as the characteristic blocking temperature of the magnetic moments of the particles in the studied sample.

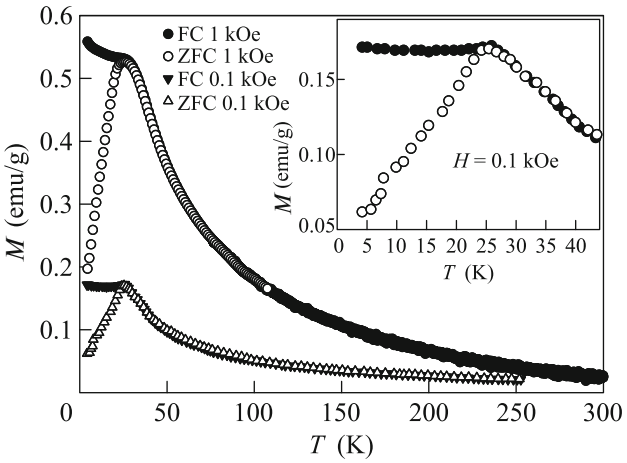

Fig. 1. Temperature dependences of the magnetization of ferrihydrite studied in the ZFC and FC modes in external fields of 0.1 and 1 kOe. The inset shows the temperature dependences $M(T)_{ZFC}$ and $M(T)_{FC}$ for $H = 0.1$ kOe on a larger scale.

Figure 2 shows the field dependences of the frequency $\nu(H)$ for temperatures of 4.2 and 150 K. It is seen that both dependences are linear, and the dependence $\nu(H)$ for $T = 4.2$ K is characterized by a gap that disappears at high temperatures. The field H^A characterizing the gap at 4.2 K is 7 kOe ($\gamma = 2.9$ GHz/kOe).

The temperature dependence of the resonance field for a frequency of 75 GHz is given in the inset of Fig. 2. It is seen that the dependence $H_R(T)$ is saturated (reaches a plateau) at the field $H_{RS} \approx 25$ kOe. Therefore, the field characterizing the gap (and, in fact, the induced anisotropy) can be determined as $H^A = H_{RS} - H_R$. According to this expression, the temperature dependences of the anisotropy field $H^A(T)$ were determined from Fig. 2 and are given in Fig. 3. It is seen that the induced anisotropy field H_R depends linearly on the temperature. The induced anisotropy tends to zero, $H^A \to 0$, at temperatures $T^* \approx 50$ and 55 K for frequencies $\nu = 52$ and 75 GHz, respectively. Thus, the field dependence of the ferromagnetic resonance (FMR) frequency is described in the studied ferrihydrite sample by the expression

$$2\pi\nu/\gamma = H_R + H^A_{(T=0)}(1 - T/T^*), \quad (1)$$

where γ is the gyromagnetic ratio, H_R is the resonance field, $H^A_{(T=0)} \approx 7$ kOe, and $T^* \approx 50$ K for a frequency of 52 GHz.

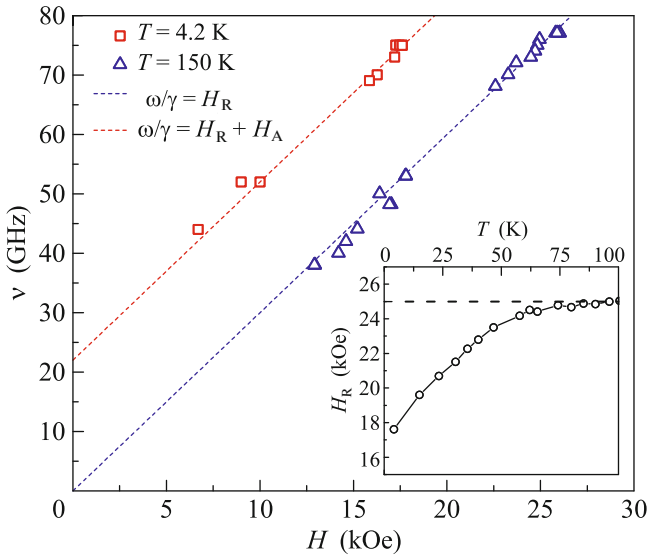

Fig. 2. (Color online) Field dependences of the frequency $\nu(H)$ for studied ferrihydrite at temperatures of 4.2 and 150 K. The inset shows the temperature dependence of the resonance field $H_R(T)$ of studied ferrihydrite at a frequency of 75 GHz.

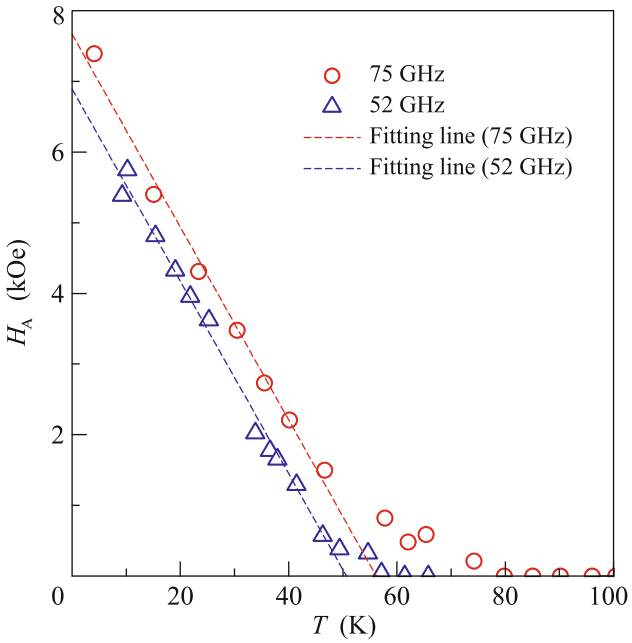

Fig. 3. (Color online) Temperature-induced anisotropy fields $H^A(T)$ of studied ferrihydrite at frequencies of $\nu = 52$ and 75 GHz.

Thus, there are several characteristic temperatures for the studied ferrihydrite nanoparticles: $T_{max} \approx 25$ K from the magnetometry data and $T^* \approx 50$ and 55 K from the magnetic resonance data at different frequencies, at which the induced anisotropy (gap) disappears. For the further analysis, we use the known Néel–Brown relation

$$k_B T = E_A / \ln(\tau_m/\tau_0) \quad (2)$$

usually used for superparamagnetic systems. Here, k_B is the Boltzmann constant; $E_A = K_{eff}V$ is the magnetic anisotropy energy, where K_{eff} is the effective magnetic anisotropy constant and V is the particle volume; τ_m is the characteristic measurement time; and τ_0 is the characteristic relaxation time of a particle. The τ_0 value may vary in the range of 10^{-13}–10^{-9} s [2], $\tau_m \sim$ 10–100 s for quasistatic magnetic measurements, and $\tau_m = 1/\nu$ is obviously for magnetic resonance. We analyze the characteristic temperatures obtained for the studied ferrihydrite sample in terms of Eq. (2). For magnetic resonance, $\tau_m = 1/\nu = 1.9 \times 10^{-11}$ and 1.33×10^{-11} s at $T^* = 50$ and 55 K, respectively. Substituting these data into Eq. (2), we obtain a system of two equations with two unknowns E_A and τ_0. The solution of this system gives $\tau_0 = 3.5 \times 10^{-13}$ s and $E_A = 2.8 \times 10^{-14}$ erg. Then, taking these E_A and τ_0 values and using $\tau_m = 100$ s for magnetic measurements, we obtain the characteristic temperature $T^* \approx 6$ K for quasistatic magnetic measurements. This is much less than the superparamagnetic blocking temperature $T_{max} = 25$ K obtained from magnetic measurements (see Fig. 1). Therefore, the gap observed under magnetic resonance conditions is due to induced anisotropy, which is not associated with blocking of the magnetic moments of the particles, but is a manifestation of another magnetic subsystem or the coupling of two magnetic subsystems. It is reasonable that the second magnetic subsystem is a subsystem of surface spins.

At the same time, the E_A value characterizing the uncompensated magnetic moment of the particle can also be obtained from the superparamagnetic blocking temperature (25 K, see Fig. 1) using Eq. (2). Since the τ_m value for magnetic measurements is large (100 s), the characteristic relaxation time τ_0 is not critical for the determination of E_A because of the logarithmic dependence in Eq. (2). At a reasonable value $\tau_0 = 10^{-11}$ s [12, 34, 35], we obtain $E_A \approx 1.03 \times 10^{-13}$ erg; this magnetic anisotropy energy now corresponds to the uncompensated moment of the core of particles, and it is several times larger than the anisotropy energy for the subsystem of surface spins.

The gap in the field dependences of the frequency $\nu(H)$ at the temperature T^* indicates the occurrence of an additional source of magnetic anisotropy. It is reasonable to associate it with the magnetic coupling energy of the subsystems of the core and surface spins. Here, H^A (≈7 kOe at $T = 0$) obtained under magnetic resonance conditions is not the exchange

bias field of the hysteresis loop, but is a field induced by the magnetic coupling of the core and "shell." A 3-nm ferrihydrite particle contains ~1000 iron atoms (the average Fe–Fe distance is ≈0.3 nm [6]) and N_S ~ 100 iron atoms on the surface. The Zeeman energy of surface atoms in the induced field can be estimated as $E_Z \approx N_S \mu_{Fe}$, where μ_{Fe} is the magnetic moment of the Fe atom ($\approx 5\mu_B$); μ_B is the Bohr magneton. This expression at $N_S = 100$ and $H^A_{(T=0)} = 7$ kOe gives $E_Z = 3.2 \times 10^{-14}$ erg, which is in good agreement with the value $E_A = 2.8 \times 10^{-14}$ erg obtained above. Thus, the subsystem of surface spins is in the induced anisotropy field caused by the coupling with the spins of the core, and this coupling occurs under magnetic resonance conditions in the temperature range below T^*. This temperature can be considered as the temperature of the transition of the subsystem of surface spins to the spin-glass state.

Drawing an analogy of nanoparticles with a core/shell structure with two-layer antiferromagnet/ferromagnet systems [36, 37], the antiferromagnetic core particles with an uncompensated magnetic moment should be identified with the ferromagnetic layer, and the spin-glass surface, with the antiferromagnet. The observed linear temperature dependence of the induced anisotropy field (Fig. 3, Eq. (1)) is consistent with the results obtained in [38] for a random field model. According to [38], the law of decreasing exchange unidirectional anisotropy with increasing temperature is determined by the type of magnetic anisotropy in the layer where the exchange spin spring is formed. Crystal systems with uniaxial and cubic anisotropies are described by the law $(1 - T/T^*)^n$ with $n = 1.5$ and 1, respectively. In other words, the law of the decrease in the exchange anisotropy is determined by the number of easy magnetization axes in the fixing layer. The larger their number, the lower the rate of decrease in the exchange energy with increasing temperature. In our case, the fixing layer is the shell in the spin-glass state, in which uniaxial anisotropy is hardly possible. Therefore, the detection of the law $H^A \sim (1 - T/T^*)^1$ is not surprising. A similar linear temperature dependence was observed in the experimental study of maghemite nanoparticles by static (magnetization) [39] and dynamic (ferromagnetic resonance) [40, 41] methods.

The temperature of the transition to the spin-glass state depends on the measurement technique. If the T^* values for magnetic resonance conditions are 50–55 K, then this temperature for quasistationary conditions (magnetization measurements) is quite low, about 6 K (the T^* value should also be determined by the magnetic field used in a particular experiment, since the magnetic field forms the magnetization of the spin-glass surface). The minimum in the dependence and a small increase in the magnetization under FC conditions in the temperature range below 10 K (see the inset of Fig. 1) may be a manifestation of the transition to the spin-glass state in magnetic measurements [6, 7].

4. CONCLUSIONS

Ferrihydrite nanoparticles of biogenic origin with a size of about 3 nm have been studied using static magnetometry and ferromagnetic resonance. Like similar objects of synthetic ferrihydrite and ferritin, the nanoparticles of the sample under study have uncompensated magnetic moments and exhibit a superparamagnetic behavior; the superparamagnetic blocking temperature for static magnetization conditions is ≈25 K. At the same time, the data of ferromagnetic resonance have indicated that the field dependences of the frequency are characterized by a gap H^A, which decreases linearly with increasing temperature according to the law $H^A_{(T=0)}(1 - T/T^*)$, where T^* depends on the frequency and ranges from 50 to 55 K (at $\nu = 52$ and 75 GHz, respectively). The analysis of the data has shown that the observed gap is associated with induced anisotropy caused by the interaction of the surface-spin subsystem with the spins of the core of the particle. The appearance of induced anisotropy at T^* corresponds to the freezing of the subsystem of surface spins and its transition to the spin-glass state under ferromagnetic resonance conditions. The linear temperature dependence of anisotropy is explained within the random field model [38] for the ferromagnet/antiferromagnet structure.

Thus, ferrihydrite nanoparticles are a good example of a core–shell magnetic structure. The exchange coupling of the spins of the core and shell leads to a spin-glass state of surface spins, which appears as a gap on the field dependence of the frequency when studying magnetic resonance.

FUNDING

This work was supported by the Russian Foundation for Basic Research, by the Government of Krasnoyarsk krai, by the Krasnoyarsk Regional Fund for the Support of Scientific and Technical Activities (project no. 19-42-240012 r_a "Magnetic Resonance in Ferrihydrite Nanoparticles: Effects Associated with the Core–Shell Structure"), and by the Council of the President of the Russian Federation for State Support of Young Scientists and Leading Scientific Schools (project no. MK-1263.2020.3).

REFERENCES

1. M. A. Chuev, I. N. Mishchenko, S. P. Kubrin, and T. A. Lastovina, JETP Lett. **105**, 700 (2017).
2. S. Morup, D. E. Madsen, C. Frandsen, C. R. H. Bahl, and M. F. Hansen, J. Phys.: Condens. Matter **19**, 213202 (2007).

3. Y. L. Raikher and V. I. Stepanov, J. Phys.: Condens. Matter **20**, 204120 (2008).
4. S. A. Makhlouf, F. T. Parker, and A. E. Berkowitz, Phys. Rev. B **55**, R14717 (1997).
5. N. J. O. Silva, V. S. Amaral, and L. D. Carlos, Phys. Rev. B **71**, 184408 (2005).
6. A. Punnoose, T. Phanthavady, M. S. Seehra, N. Shah, and G. P. Huffman, Phys. Rev. B **69**, 54425 (2004).
7. M. S. Seehra, V. Singh, X. Song, S. Bali, and E. M. Eyring, J. Phys. Chem. Solids **71**, 1362 (2010).
8. S. I. Popkov, A. A. Krasikov, D. A. Velikanov, V. L. Kirillov, O. N. Martyanov, and D. A. Balaev, J. Magn. Magn. Mater. **483**, 21 (2019).
9. Y. V. Knyazev, D. A. Balaev, V. L. Kirillov, O. A. Bayukov, and O. N. Mart'yanov, JETP Lett. **108**, 527 (2018).
10. R. H. Kodama and A. E. Berkowitz, Phys. Rev. B **59**, 6321 (1999).
11. T. Hiemstra, Geochim. Cosmochim. Acta **158**, 179 (2015).
12. M. S. Seehra, V. S. Babu, A. Manivannan, and J. W. Lynn, Phys. Rev. B **61**, 3513 (2000).
13. S. V. Stolyar, R. N. Yaroslavtsev, R. S. Iskhakov, O. A. Bayukov, D. A. Balaev, A. A. Dubrovskii, A. A. Krasikov, V. P. Ladygina, A. M. Vorotynov, and M. N. Volochaev, Phys. Solid State **59**, 555 (2017).
14. S. V. Stolyar, D. A. Balaev, A. A. Krasikov, A. A. Dubrovskiy, R. N. Yaroslavtsev, O. A. Bayukov, M. N. Volochaev, and R. S. Iskhakov, J. Supercond. Nov. Magn. **31**, 1133 (2018).
15. D. A. Balaev, A. A. Krasikov, A. A. Dubrovskiy, S. I. Popkov, S. V. Stolyar, R. S. Iskhakov, V. P. Ladygina, and R. N. Yaroslavtsev, J. Appl. Phys. **120**, 183903 (2016).
16. E. Wajnberg, L. J. El-Jaick, M. P. Linhares, and D. M. S. Esquivel, J. Magn. Reson. **153**, 69 (2001).
17. M. P. Weir, T. J. Peters, and J. F. Gibson, Biochim. Biophys. Acta **828**, 298 (1985).
18. A. Punnoose, M. S. Seehra, J. van Tol, and L. C. Brunel, J. Magn. Magn. Mater. **288**, 168 (2005).
19. F. Baldi, A. Minacci, M. Pepi, and A. Scozzafava, FEMS Microbiol. Ecol. **36**, 169 (2001).
20. S. V. Stolyar, O. A. Bayukov, Y. L. Gurevich, E. A. Denisova, R. S. Iskhakov, V. P. Ladygina, A. P. Puzyr', P. P. Pustoshilov, and M. A. Bitekhtina, Inorg. Mater. **42**, 763 (2006).
21. S. Kianpour, A. Ebrahiminezhad, M. Mohkam, A. M. Tamaddon, A. Dehshahri, R. Heidari, and Y. Ghasemi, J. Basic Microbiol. **57**, 132 (2017).
22. S. V. Stolyar, O. A. Bayukov, D. A. Balaev, R. S. Iskhakov, L. A. Ishchenko, V. P. Ladygina, and R. N. Yaroslavtsev, J. Optoelectron. Adv. Mater. **17**, 968 (2015).
23. V. P. Ladygina, K. V. Purtov, S. V. Stoljar, R. S. Iskhakov, O. A. Bajukov, J. L. Gurevich, K. G. Dobretsov, and L. A. Ishchenko, Patent No. EA018956 (2013).
24. L. Anghel, M. Balasoiu, L. A. Ishchenko, S. V. Stolyar, T. S. Kurkin, A. V. Rogachev, A. I. Kuklin, Y. S. Kovalev, Y. L. Raikher, R. S. Iskhakov, and G. Duca, J. Phys.: Conf. Ser. **351**, 12005 (2012).
25. D. A. Velikanov, Sib. J. Sci. Technol. **2** (48), 176 (2013).
26. V. I. Tugarinov, I. Y. Makievskii, and A. I. Pankrats, Instrum. Exp. Tech. **47**, 472 (2004).
27. S. V. Stolyar, D. A. Balaev, V. P. Ladygina, et al., J. Supercond. Nov. Magn. **31**, 2297 (2018).
28. D. A. Balaev, A. A. Krasikov, A. A. Dubrovskiy, S. I. Popkov, S. V. Stolyar, O. A. Bayukov, R. S. Iskhakov, V. P. Ladygina, and R. N. Yaroslavtsev, J. Magn. Magn. Mater. **410**, 171 (2016).
29. S. V. Stolyar, O. A. Bayukov, Y. L. Gurevich, V. P. Ladygina, R. S. Iskhakov, and P. P. Pustoshilov, Inorg. Mater. **43**, 638 (2007).
30. D. A. Balaev, A. A. Dubrovskii, A. A. Krasikov, S. V. Stolyar, R. S. Iskhakov, V. P. Ladygina, and E. D. Khilazheva, JETP Lett. **98**, 139 (2013).
31. D. A. Balaev, S. I. Popkov, A. A. Krasikov, A. D. Balaev, A. A. Dubrovskiy, S. V. Stolyar, R. N. Yaroslavtsev, V. P. Ladygina, and R. S. Iskhakov, Phys. Solid State **59**, 1940 (2017).
32. D. A. Balaev, A. A. Krasikov, A. A. Dubrovskii, S. V. Semenov, O. A. Bayukov, S. V. Stolyar, R. S. Iskhakov, V. P. Ladygina, and L. A. Ishchenko, J. Exp. Theor. Phys. **119**, 479 (2014).
33. C. G. Chilom, D. M. Gazdaru, M. Balasoiu, M. Bacalum, S. V. Stolyar, and A. I. Popescu, Rom. J. Phys. **62**, 701 (2017).
34. E. L. Duarte, R. Itri, E. Lima, M. S. Baptista, T. S. Berqué, and G. F. Goya, Nanotechnology **17**, 5549 (2006).
35. T. S. Berqué, J. J. Erbs, A. Lindquist, R. L. Penn, and S. K. Banerjee, J. Phys.: Condens. Matter **21**, 176005 (2009).
36. J. Nogues, J. Sort, V. Langlais, V. Skumryev, S. Suriñach, J. S. Muñoz, and M. D. Baro, Phys. Rep. **422** (3), 65 (2005).
37. J. Nogues and I. K. Schuller, J. Magn. Magn. Mater. **192**, 203 (1999).
38. A. P. Malozemoff, J. Appl. Phys. **63**, 3874 (1988).
39. B. Martinez, X. Obradors, L. Balcells, A. Rouanet, and C. Monty, Phys. Rev. Lett. **80**, 181 (1998).
40. E. Winkler, R. D. Zysler, M. V. Mansilla, and D. Fiorani, Phys. Rev. B **72**, 132409 (2005).
41. Y. A. Koksharov, S. P. Gubin, I. D. Kosobudsky, G. Y. Yurkov, D. A. Pankratov, L. A. Ponomarenko, M. G. Mikheev, M. Beltran, Y. Khodorkovsky, and A. M. Tishin, Phys. Rev. B **63**, 12407 (2000).

Translated by L. Mosina